Nano Energy (2013) 2, 1093–1100

Available online at www.sciencedirect.com

ScienceDirect

journal homepage: www.elsevier.com/locate/nanoenergy

RAPID COMMUNICATION

Effective piezo-phototronic enhancement of solar cell performance by tuning material properties

Xiaonan Wen[a], Wenzhuo Wu[a], Zhong Lin Wang[a,b,*]

[a]School of Materials Science and Engineering, Georgia Institute of Technology, Atlanta, GA 30332-0245, USA
[b]Satellite Research Facility, MANA, International Center for Materials Nanoarchitectonics, National Institute for Materials Science, 1-1 Namiki, Tsukuba 305-0044, Japan

Received 27 August 2013; accepted 30 August 2013
Available online 16 September 2013

KEYWORDS
Piezo-phototronics;
Solar cell;
ZnO

Abstract
Piezo-phototronic effect is demonstrated in the ZnO/P3HT solar cell system and detailed study is conducted regarding the influence of crystallization and doping level of ZnO on the strength of piezo-phototronic effect as well as the overall solar cell performance. By testing and comparing five groups of samples prepared under different conditions, optimized parameters are determined for the most efficient piezo-phototronic enhancement of solar cell performance. The general principles and regularities provided in this study are universal and applicable to all solar cell systems involving piezoelectric semiconductor materials and could provide substantial guidance on further increasing performances of commercial solar cells based on CdTe, GaAs etc. and also spur the development of flexible solar cells for smart applications in various situations.
© 2013 Elsevier Ltd. All rights reserved.

Introduction

Wurtzite and Sphalerite semiconductors such as GaN, InN, ZnO, CdTe have outstanding electrical and optical properties and are excellent materials for optoelectronic applications [1–5]. However, one of their properties, the piezoelectricity, was largely neglected owing to their superior optoelectronic applications. Only until recently, it was suggested that the presence of polarization charges at contact interfaces, such as p-n junctions and Schottky junctions, could significantly impact the performance of optoelectronic devices [6–12]. In short, the effect, which is named as the piezo-phototronic effect, describes the phenomenon that the efficiency of charge generation, separation or recombination is tuned by the polarization charges at the interface, and the performance of optoelectronic devices can be either enhanced or degraded

*Corresponding author at: School of Materials Science and Engineering, Georgia Institute of Technology, Atlanta, GA 30332-0245, USA.
E-mail address: zhong.wang@mse.gatech.edu (Z.L. Wang).

2211-2855/$ - see front matter © 2013 Elsevier Ltd. All rights reserved.
http://dx.doi.org/10.1016/j.nanoen.2013.08.008

depending on the sign of the charges [13-16]. This effect opens up a new field for science and technological applications.

Solar cells, among the most important types of optoelectronic devices, have been intensively studied these years as a potential solution to the energy crisis and environmental pollution. Most research efforts are focused on promoting its energy conversion efficiency [17-19], which is related to factors like reflection, electrical resistance, carrier separation, recombination etc. and there are also increasing interests in flexible and smart applications of solar cells in various situations [20-23]. Piezo-polarization charges at p-n junction interface directly interfere with the separation and recombination process and it has been theoretically predicted [24,25] as well as experimentally proved [9,10,26] that the effect does affect solar cell efficiencies. However, all of previous studies were limited to demonstrating the effect itself without providing further guidance on how the selection of materials and tuning of material properties can strengthen the piezo-phototronic effect and whether the strengthening of piezo-phototronic effect could always be beneficial for solar cell performances.

To answer the above questions, we took the ZnO/P3HT solar cell system as an example and detailedly studied on how the material properties of crystallization and doping level affect the piezo-phototronic effect and to what level the improvement of said effect affects the original strain-free solar cell performance. The results provided in this study are not limited to ZnO/P3HT and is universal and applicable to all solar cell systems involving piezoelectric semiconductor materials. This study is not only significant to development of important commercialized solar cells made of CdTe, GaAs on hard substrates, where pre-straining could be engineered into piezoelectric layers, but also beneficial to the development of inorganic/organic hybrid solar cells that are flexible, inexpensive and easily scalable.

Methods

The structure of the solar cell is shown in Fig. 1(a). 100 nm of ITO is firstly deposited onto transparent and flexible PET substrate as the top electrode. 600 nm of ZnO is subsequently deposited using an RF sputterer, leaving out the margins for later electric connection. The sputtering parameters vary for different groups of samples according to the needs of our study but the common parameters are a RF power of 120 W and a total pressure of 6 mTorr during the deposition. Electronic grade P3HT was purchased from Sigma-Aldrich and dissolved into chlorobenzene at a concentration of 10 mg/ml without further purification. Then the solution is spin coated onto the ZnO layer at a speed of 700 rpm for 30 s to form the p-type layer. Drying is subsequently performed at 120 °C for 5 min under nitrogen environment to improve the electrical and contact properties. Lastly, a 100 nm gold layer is deposited on P3HT as the bottom electrode.

Results and discussion

A solar simulator (Model 91160, Newport, 300 W, AM 1.5) is used to provide illumination to the solar cells with its output power adjusted to 100 mW/cm^2, which is considered the

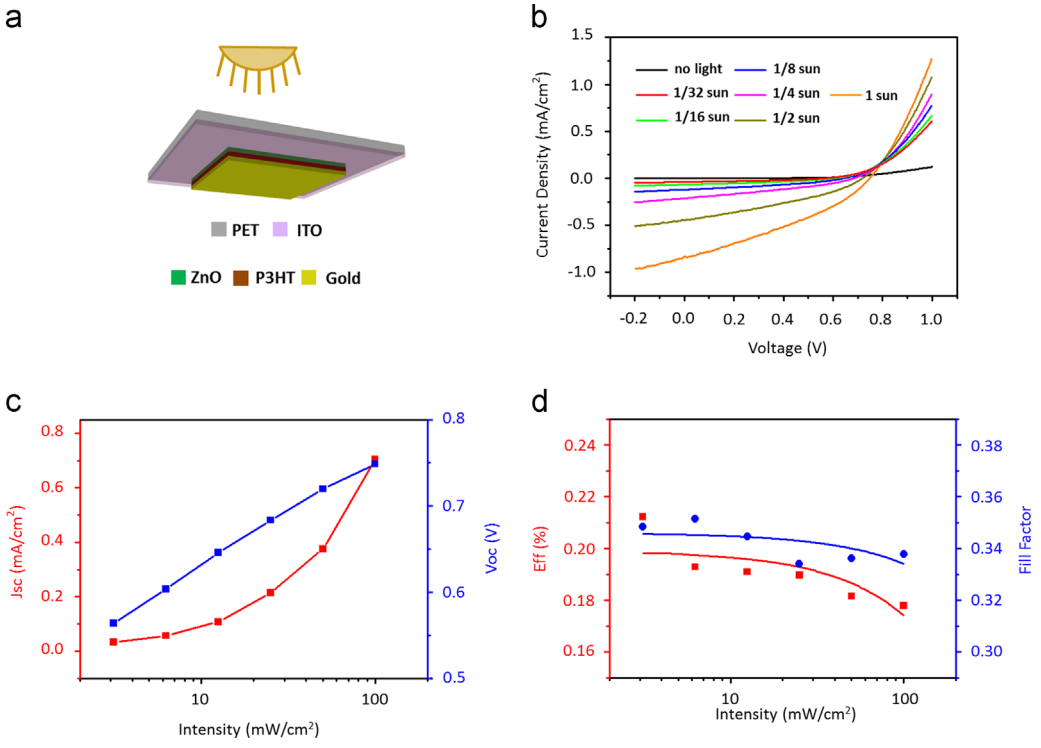

Fig. 1 General performance of strain-free ZnO/P3HT solar cell (Group 1) is shown in this figure. (a) Schematic of the solar cell structure. (b) *J*-*V* characteristics of the solar cell under different illumination intensities, from one full sun (100 mW/cm^2) to as low as 1/32 sun (3.125 mW/cm^2). (c) J_{SC} and V_{OC} of the solar cell under different illumination intensities. *X*-axis values are expressed in log 10 scale. (d) Efficiency and fill factor under different illumination intensities. Data points are linearly fitted. *X*-axis values are expressed in log 10 scale.

intensity of one sun under normal conditions. A set of sunlight attenuators is used to achieve different levels of illumination intensity. The first solar cell sample under test is labeled as Group 1, of which the ZnO layer is sputtered at room temperature (without purposefully heating the substrate during sputtering) with Ar flow rate at 30 sccm and O_2 flow rate at 10 sccm. As-measured *J*-*V* characteristics of the solar cell under 6 different illumination intensities are shown in Fig. 1(b). At 100 mW/cm^2, the solar cell yields an open-circuit voltage (V_{OC}) of 0.7487 V, a short-circuit current density (J_{SC}) of 0.7036 mA/cm^2, a fill factor of 0.3378 and an efficiency of 0.178%. When the illumination intensity is decreased to 3.125 mW/cm^2, the solar cell yields a V_{OC} of 0.5641 V, a J_{SC} of 0.0336 mA/cm^2, a fill factor of 0.3484 and an efficiency of 0.212%. The values of V_{OC} and J_{SC} under different intensities are summarized in Fig. 1 (c) and the values of efficiency and fill factor under different intensities are summarized in Fig. 1(d), indicating that the efficiency of the solar cell increases with lowering illumination intensities. This phenomenon could be explained by its limited charge separation ability meaning that under a higher generation rate, the proportion of electron-hole pairs that can be separated by the junction region is lower. In the following, the method to improve this ability will be demonstrated and discussed.

The performance of Group 1 solar cell under strains at the illumination intensity of 25 mW/cm^2 (the rest of the measurements will all be done at this intensity) is subsequently tested. Before strain is loaded, the solar cell yields a J_{SC} of 0.2150 mA/cm^2, a V_{OC} of 0.6823 V and an efficiency of 0.188%. After strain is applied (method shown in the inset of Fig. 2(a)), we observe increases in J_{SC} under tensile strain and decreases in J_{SC} under compressive strain (tensile strain is defined as positive and compressive strain is defined as negative; strain values are calculated according to previous studies [27,28]) but the V_{OC} almost remains unaffected, as is shown in the *J*-*V* characteristics in Fig. 2 (a). Specifically, the J_{SC} experiences a 2.568% increase to 0.2205 mA/cm^2 under 0.32% tensile strain and a 4.940% decrease to 0.2042 mA/cm^2 under 0.32% compressive strain. Accordingly, the efficiency is increased by 3.456% to 0.194% under 0.32% tensile strain and is decreased by 2.432% to 0.183% under 0.32% compressive strain (relevant data will be summarized in Fig. 5). Since RF-sputtered ZnO film is self-textured [29-31], the asymmetry of performance change by loading opposite signs of strain clearly suggests that piezoelectricity plays a role in the process. A model is presented in Fig. 2(b) to explain the performance change. The band structure for the strain free condition is shown in Fig. 2(b1). The basic processes for a solar cell to work are the generation of electron-hole pairs, separation of electron-hole pairs and recombination of those carriers in external circuits. The step of critical importance here is the electron-hole pair separation. For J_{SC}, its value is directly related to the carrier collection probability. Qualitatively, a stronger built-in field in the junction region means a higher collection probability for the carriers and vice versa. When external strain is applied to the ZnO thin film, creating negative polarization charges at the ZnO/P3HT interface, both the conduction and valence bands in the junction region will be lifted up, weakening the strength of the built-in field and leading to

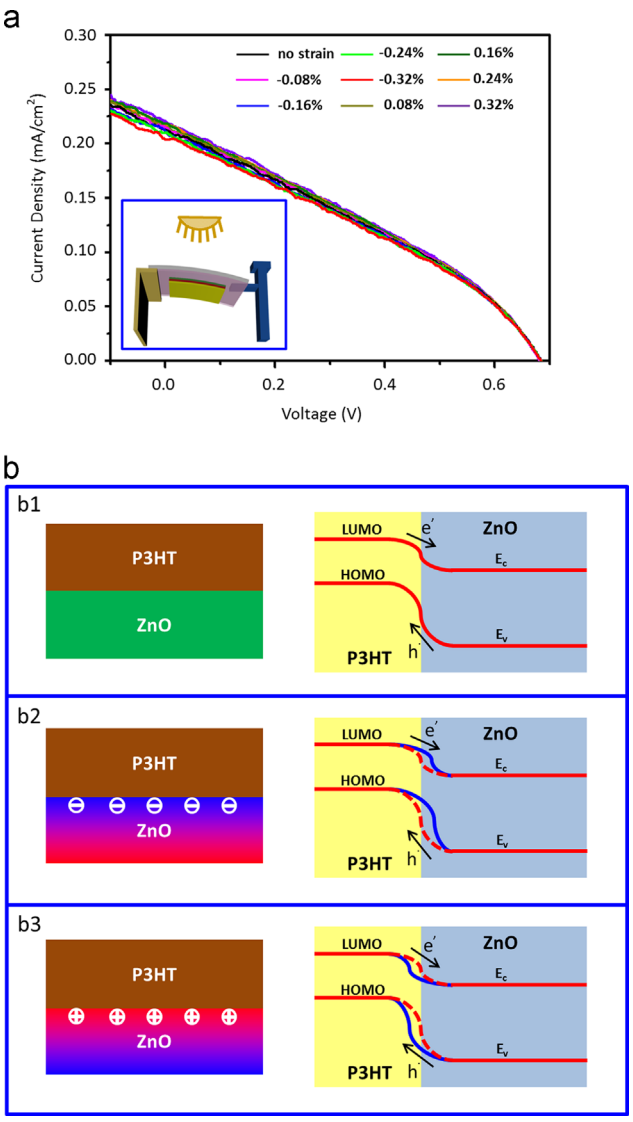

Fig. 2 Group 1 solar cell performance under strains and the mechanism for piezo-phototronic effect. (a) *J*-*V* characteristics of Group 1 solar cell under strains at the illumination intensity of 25 mW/cm^2. The inset shows the method to apply strain to the solar cell. (b) Schematics explaining the mechanism how piezo-phototronic effect tunes the solar cell performance. Red line represents the band structure without strain. Blue line represents the tuned band structure with strain.

a decrease of J_{SC}. On the contrary, positive polarization charges created at the interface will lower the conduction and valence bands in the junction region, strengthening the built-in field and result in an increase of J_{SC}. As for the V_{OC}, its value is determined by the difference between quasi-Fermi levels of the p-type and n-type semiconductor, which is largely decided by the illumination intensity. Quantitatively, $V_{OC} \approx (nkT/q)Ln(J_{SC}/J_O)$ (n is the ideality factor, kT/q is the thermal voltage and J_O is the dark reserve saturated current), which means the change in J_{SC} does affect the value of V_{OC}. However, since $d(V_{OC}) \approx (nkTJ_O/q)(d(J_{SC})/J_{SC})$, (the value of nkT/q is on the order of 30 mV and the value of J_{SC}/J_O is $\sim$250 according to Fig. 1

(b)), 1 mA/cm^2 change in J_{SC} only leads to approximately 1.2×10^{-4} V variation in V_{OC} and can thus be considered negligible. This explains why on the *J*-*V* characteristic of Fig. 2(a), the voltage stays mostly unaffected by the strains.

Although the piezo-phototronic effect demonstrated for Group 1 sample can indeed improve or degrade the solar cell performance, the amount of change is relatively small and we need to look for methods to further improve this effect. As is shown by many studies [29-33], the piezoelectricity in sputtered ZnO film arises from the *c*-axis self-aligning among grains and one way to increase its piezoelectric coefficient is to improve the crystallinity by thermal processing. Thus in Group 2 sample, the ZnO is deposited when the sample substrate is heated at 120 °C during the whole sputtering process while all other parameters are kept the same as for Group 1. X-ray Diffraction (XRD) technique is used to analyze the as-sputtered ZnO and determine the level of alignment. As indicated in Fig. 3(a), both samples have a diffraction peak at $2\theta \approx 34°$, corresponding to the (0002) plane of Wurtzite ZnO (the plane that is responsible for the piezoelectric property). It is clearly shown that the

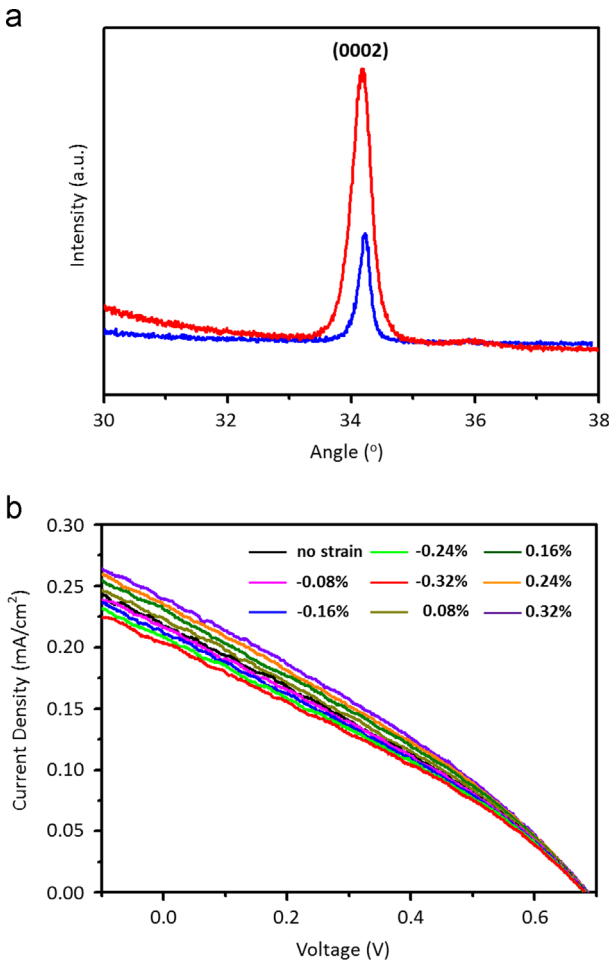

Fig. 3 Effect of thermal processing on the strength of piezo-phototronic effect and the solar cell performance. (a) XRD spectrum for Group 1 sample, in blue, and Group 2 sample, in red. (b) *J*-*V* characteristics of Group 2 solar cell under strains at the illumination intensity of 25 mW/cm^2.

Group 2 sample, represented by the red curve, has a higher level of alignment and thus a higher piezoelectric coefficient compared to Group 1 sample, represented by the blue curve. Group 2 solar cell is subsequently tested under different strain levels and the *J*-*V* characteristics are plotted in Fig. 3(b). Under zero strain, the J_{SC} is 0.217 mA/cm^2, the V_{OC} is 0.683 V and the efficiency is 0.18%. Inevitably, the electrical properties of Group 2 ZnO will be different from Group 1 due to slight difference in factors like grain size but in general, the thermal processing can be considered to have little influence on the performance of strain free solar cells. When strain is applied to the Group 2 device, we observe a much higher level of change on the solar cell performance. Specifically, J_{SC} is increased by 9.96% to 0.239 mA/cm^2 under 0.32% tensile strain and is decreased by 6.292% to 0.204 mA/cm^2 under 0.32% compressive strain. Accordingly, the efficiency is increased by 12.1% to 0.203% under 0.32% tensile strain and is decreased by 6.84% to 0.169% under 0.32% compressive strain (relevant data will be summarized in Fig. 5). Thus, by comparing the measurement results from Group 1 and Group 2, it can be concluded that thermal processing, which improves the crystallinity and piezoelectric strength of ZnO film, is an effective method to enhance the piezo-phototronics effect without degrading the original performance of strain-free solar cells.

Different from conventional piezoelectric materials such as PZT, $BaTiO_3$ which are insulators, free charge carriers in piezoelectric semiconductors can always partially screen the piezopotential, thus weakening the piezoelectric output. Therefore, in addition to improving crystallinity of ZnO, reducing the doping concentration will also improve piezo-phototronic effect. However, compared to crystallinity which has little impact on semiconducting properties if well controlled, adjustment of doping level almost certainly affects solar cell performance. It is sophisticated to tell whether the doping level change lowers the solar cell performance, and if it does, whether the loss could be compensated by the performance enhancement from piezo-phototronics effect. To answer the above question, several groups of samples will be studied below.

As many studies suggest [34-36], the doping level of ZnO is closely related to the atmosphere during sputtering and a lower partial pressure of oxygen will give rise to a higher level of oxygen vacancies and therefore a higher doping level. ZnO layer of the first sample under test in this section is sputtered with pure Ar at a flow rate of 40 sccm under 120 °C substrate heating, labeled as Group 3. The as-measured *J*-*V* characteristics are shown in Fig. 4(a). In strain free condition, the solar cell yields a J_{SC} of 0.1176 mA/cm^2, a V_{OC} of 0.374 V and an efficiency of 0.05%. When strain is applied, we see a similar trend of performance tuning. Specifically, J_{SC} is increased by 8.58% to 0.1277 mA/cm^2 under 0.32% tensile strain and is decreased by 9.50% to 0.1065 mA/cm^2 under 0.32% compressive strain. Accordingly, the efficiency is increased by 9.3% to 0.056% under 0.32% tensile strain and is decreased by 8.53% to 0.047% under 0.32% compressive strain. For comparison purpose, the *J*-*V* characteristics of Group 2 sample (30 sccm Ar, 10 sccm O_2, substrate heated at 120 °C), which was discussed above, is also shown in Fig. 4(b). Then to further increase the oxygen partial pressure, ZnO of Group 4 is sputtered under 20 sccm of Ar and 20 sccm of O_2,

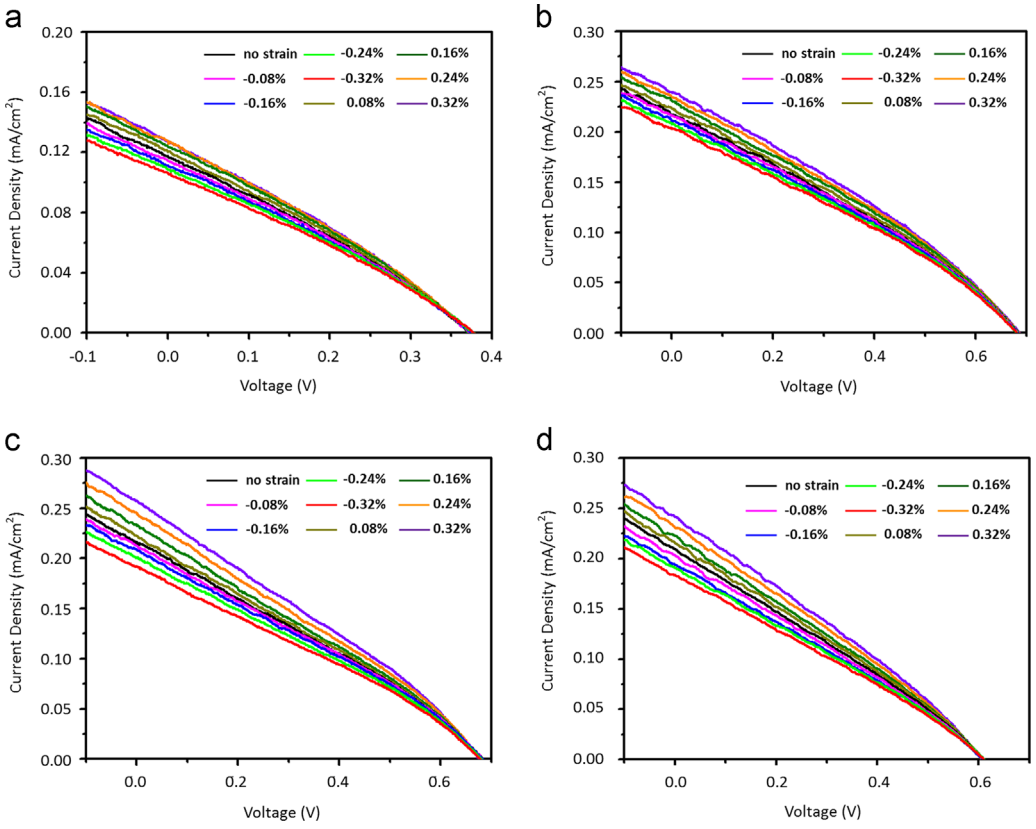

Fig. 4 Effect of sputtering atmosphere on the strength of piezo-phototronic effect and the solar cell performance. (a) *J*-*V* characteristics of Group 3 solar cell under strains at the illumination intensity of 25 mW/cm^2. (b) *J*-*V* characteristics of Group 2 solar cell under strains at the illumination intensity of 25 mW/cm^2. (c) *J*-*V* characteristics of Group 4 solar cell under strains at the illumination intensity of 25 mW/cm^2. (d) *J*-*V* characteristics of Group 5 solar cell under strains at the illumination intensity of 25 mW/cm^2.

heated at 120 °C. Shown by the *J*-*V* characteristics in Fig. 4 (c), at zero strain, the solar cell yields a J_{SC} of 0.2153 mA/cm^2, a V_{OC} of 0.683 V and an efficiency of 0.17%. When 0.32% tensile strain is applied, J_{SC} is increased by 19.97% to 0.258 mA/cm^2 and efficiency is increased by 17.1% to 0.2%. When 0.32% compressive strain is applied, J_{SC} is decreased by 11.2% to 0.191 mA/cm^2 and efficiency is decreased by 9.16% to 0.155%. ZnO layer of the last group is sputtered under 10 sccm of Ar and 30 sccm of O_2, heated at 120 °C and the solar cell *J*-*V* characteristics are shown in Fig. 4(d). At zero strain, the solar cell yields a J_{SC} of 0.2095 mA/cm^2, a V_{OC} of 0.61 V and an efficiency of 0.14%. When 0.32% tensile strain is applied, J_{SC} is increased by 15.45% to 0.24 mA/cm^2 and efficiency is increased by 17.46% to 0.167%. When 0.32% compressive strain is applied, J_{SC} is decreased by 12.52% to 0.1833 mA/cm^2 and efficiency is decreased by 12.11% to 0.1248%. From the above results, we can see that oxygen partial pressure during ZnO sputtering is positively related to the strength of the piezo-phototronic effect. However, its impact on solar cell performance is rather complex.

To fully analyze and better understand the above data, J_{SC}, V_{OC}, efficiency and fill factor of all five groups of samples under 9 different strain states are summarized in Fig. 5(a)-(d) respectively. At zero strain, Group 3 has the lowest J_{SC}, V_{OC} and efficiency of all. This indicates that when ZnO is deposited under pure Ar, the doping level may be excessively high and there is significant damage to the crystal, leading to a shorter diffusion length, a higher recombination rate and a lower collection probability [37]. Group 1, 2 and 4 in the zero strain case have almost the same J_{SC} and V_{OC}. However, Group 1 enjoys the highest fill factor while Group 4 suffers the lowest fill factor, making Group 1 the most efficient solar cell under zero strain. The lowering of fill factor could be explained by the increase of series resistance [37] due to the heating of the sample and a higher oxygen partial pressure during the sputtering process. However, the level of series resistance has not yet affected the value of J_{SC} in these samples. ZnO of Group 5 is deposited under the highest oxygen partial pressure of 75%, leading to two effects. The first one is a further increase in series resistance which is possibly responsible for a lower J_{SC} compared to Group 1, 2 and 4 [37]. The second one is a decrease in shunt resistance that is reflected in its lower V_{OC} [37]. This could be attributed to the phenomenon that when an excessively high oxygen partial pressure is in presence during ZnO sputtering, surface smoothness is drastically degraded [38,39], which leads to more contact defects between ZnO and the spin-coated P3HT. When strain is gradually applied, J_{SC} and efficiency gradually increases under tensile strain and gradually decreases under compressive strain for all cases as a result of piezo-phototronic effect. On the other hand, the values of V_{OC} for all five groups stay relatively constant under different strains, reason of which has been explained above. Furthermore,

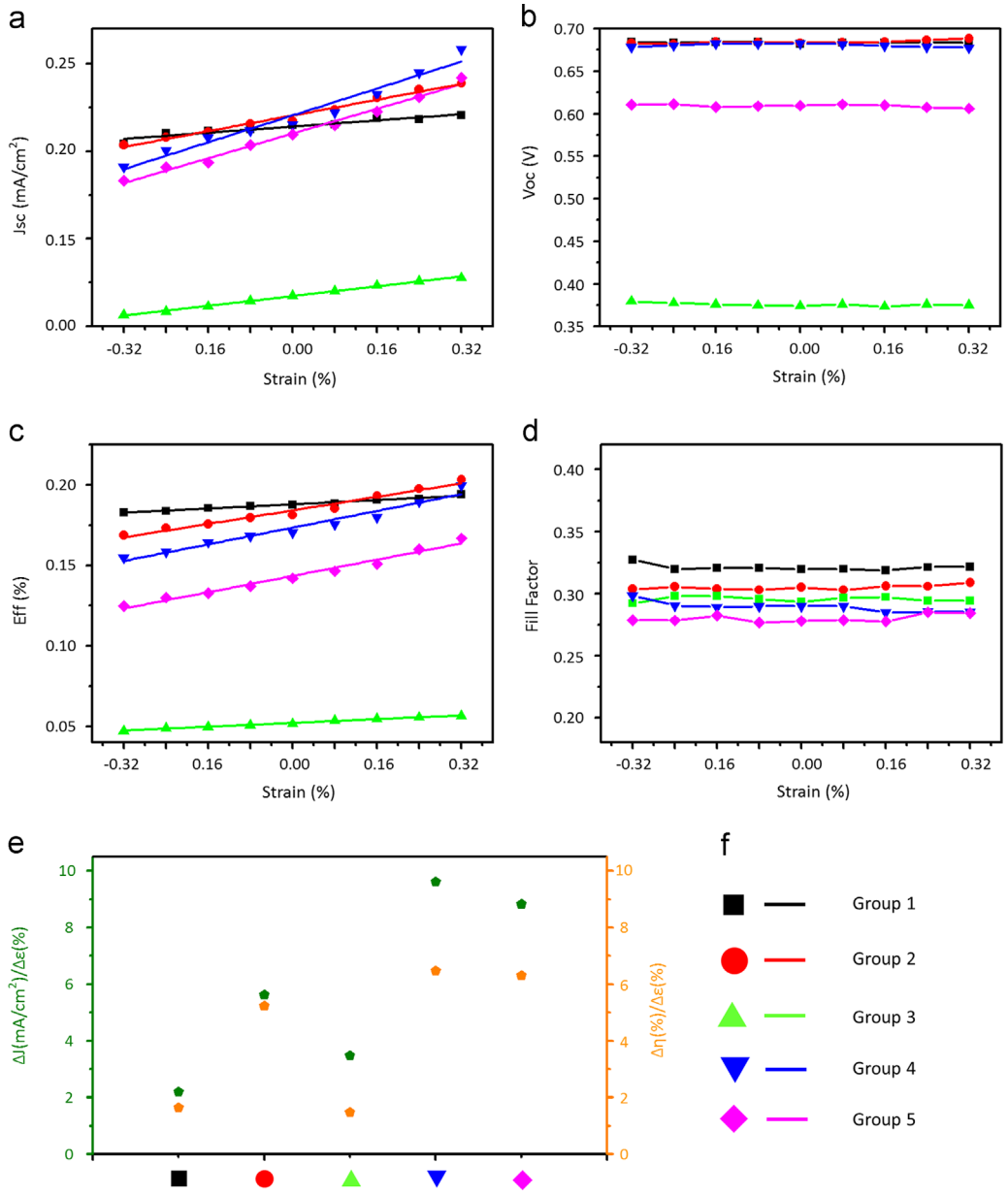

Fig. 5 Summarization of important solar cell parameters for the five groups of samples. (a) Strain – J_{sc} scattergram. Linear fitting is performed for each group. (b) Strain – V_{OC} scattergram. (c) Strain – efficiency scattergram. Linear fitting is performed for each group. (d) Strain – fill factor scattergram. (e) Scattergram for the slopes of fitted curves in (a) and (c). ε represent strain and η represent efficiency in this figure. (f) Specific symbols and colors are assigned to represent each group.

the fill factor is also stable over different strains, meaning the straining process does not impact the series and shunt resistance to an observable extent. The highest J_{SC} is achieved by Group 3 under 0.32% tensile strain thanks to the strong piezo-phototronic effect for this sample. The highest efficiency, however, is achieved by Group 2 under 0.32% since it has a higher fill factor as discussed above. To have a more direct sense of the strength of piezo-phototronic effect, J_{SC} data in Fig. 5(a) and efficiency data in Fig. 5 (c) are linearly fitted for each group. Slope values for the fitted curves in Fig. 5(a) are 2.20, 5.63, 3.47, 9.61 and 8.84 in the unit of mA/cm^2/%strain for Group 1-5, respectively, and slope values for fitted curves in Fig. 5(c) are 1.63, 5.24, 1.47, 6.48 and 6.32 in the unit of %eff/%strain for Group 1-5, respectively. These values are compiled in Fig. 5(e). As expected, under the same atmosphere, Group 2 has a larger slope for both J_{SC} and efficiency than Group 1 due to a better *c*-axis alignment. Under the same sputtering temperature the slopes of fitted curves increase with the increase of oxygen partial pressure but is saturated somewhere between 50% and 75% of oxygen partial pressure. It is worth noting that the crystallinity is not completely independent of the sputtering atmosphere and an excessively high oxygen partial pressure may lead to poorer grain alignment [38,40,41], consistent with our data showing that the curve for Group 5 has slightly smaller slopes than that of Group 4. Consequently, without taking into account of the strain-free solar cell performance, the largest amount of

performance improvement is achieved by the Group 4 sample.

Summary

In summary, the piezo-phototronic effect is demonstrated in the ZnO/P3HT solar cell system, and we have detailedly studied the influence of crystallization and doping level of ZnO on the strength of piezo-phototronic effect as well as the overall solar cell performance by testing and comparing five different groups of samples. Within our range of study, the highest efficiency is achieved by Group 2 solar cell (ZnO is sputtered at 120 W, 6 mTorr, 30 sccm Ar, 10 sccm O_2 and substrate heated to 120 °C) under 0.32% tensile strain. Further increasing the piezo-phototronic effect by using a higher oxygen partial pressure will lead to poorer strain-free solar cell performance which could not be effectively compensated by the current range of strain-induced enhancement. (However, more enhancement could be achieved by introducing a larger strain.) The general principles and regularities provided in this study are universal and applicable to all solar cell systems involving piezoelectric semiconductor materials and could provide meaningful guidance on further increasing performances of commercial solar cells based on CdTe, GaAs etc. and also spur the development of flexible solar cells for smart applications in various situations.

Acknowledgments

This work was supported by U.S. Department of Energy, Office of Basic Energy Sciences (DE-FG02-07ER46394), ARO MURI, NSF, MANA, National Institute For Materials, Japan, a joint project with Sungkyunkwan University, Korea.

References

[1] S. Xu, C. Xu, Y. Liu, Y.F. Hu, R.S. Yang, Q. Yang, J.H. Ryou, H.J. Kim, Z. Lochner, S. Choi, R. Dupuis, Z.L. Wang, Advanced Materials 22 (2010) 4749.
[2] M.H. Huang, S. Mao, H. Feick, H.Q. Yan, Y.Y. Wu, H. Kind, E. Weber, R. Russo, P.D. Yang, Science 292 (2001) 1897.
[3] F.A. Ponce, D.P. Bour, Nature 386 (1997) 351.
[4] J. Britt, C. Ferekides, Applied Physics Letters 62 (1993) 2851.
[5] A.G. Bhuiyan, A. Hashimoto, A. Yamamoto, Journal of Applied Physics 94 (2003) 2779.
[6] Q. Yang, W.H. Wang, S. Xu, Z.L. Wang, Nano Letters 11 (2011) 4012.
[7] Q. Yang, X. Guo, W.H. Wang, Y. Zhang, S. Xu, D.H. Lien, Z.L. Wang, Acs Nano 4 (2010) 6285.
[8] Q. Yang, Y. Liu, C.F. Pan, J. Chen, X.N. Wen, Z.L. Wang, Nano Letters 13 (2013) 607.
[9] C.F. Pan, S.M. Niu, Y. Ding, L. Dong, R.M. Yu, Y. Liu, G. Zhu, Z.L. Wang, Nano Letters 12 (2012) 3302.
[10] J. Shi, P. Zhao, X.D. Wang, Advanced Materials 25 (2013) 916.
[11] F. Zhang, Y. Ding, Y. Zhang, X.L. Zhang, Z.L. Wang, Acs Nano 6 (2012) 9229.
[12] W. Wu, X. Wen, Z.L. Wang, Science 340 (2013) 952.
[13] Z.L. Wang, Advanced Materials 24 (2012) 4630.
[14] Z.L. Wang, Advanced Materials 24 (2012) 4632.
[15] Z.L. Wang, Journal of Physical Chemistry Letters 1 (2010) 1388.
[16] Z.L. Wang, MRS Bulletin 37 (2012) 814.
[17] J.H. Zhao, A.H. Wang, M.A. Green, F. Ferrazza, Applied Physics Letters 73 (1998) 1991.
[18] J. Yang, A. Banerjee, S. Guha, Applied Physics Letters 70 (1997) 2975.
[19] T. Aramoto, S. Kumazawa, H. Higuchi, T. Arita, S. Shibutani, T. Nishio, J. Nakajima, M. Tsuji, A. Hanafusa, T. Hibino, K. Omura, H. Ohyama, M. Murozono, Japanese Journal of Applied Physics 1 1997, 36, 6304.
[20] Y.G. Wei, C. Xu, S. Xu, C. Li, W.Z. Wu, Z.L. Wang, Nano Letters 10 (2010) 2092.
[21] D. Kuang, J. Brillet, P. Chen, M. Takata, S. Uchida, H. Miura, K. Sumioka, S.M. Zakeeruddin, M. Gratzel, ACS Nano 2 (2008) 1113.
[22] D.J. Lipomi, B.C.K. Tee, M. Vosgueritchian, Z.N. Bao, Advanced Materials 23 (2011) 1771.
[23] Z.L. Wang, W.Z. Wu, Angewandte Chemie International Edition 51 (2012) 11700.
[24] F. Boxberg, N. Sondergaard, H.Q. Xu, Nano Letters 10 (2010) 1108.
[25] Y. Zhang, Y. Liu, Z.L. Wang, Advanced Materials 23 (2011) 3004.
[26] Y. Yang, W.X. Guo, Y. Zhang, Y. Ding, X. Wang, Z.L. Wang, Nano Letters 11 (2011) 4812.
[27] R.W. Soutas-Little, Elasticity, Dover Publications, Mineola, NY, 1999.
[28] W.Z. Wu, Y.G. Wei, Z.L. Wang, Advanced Materials 22 (2010) 4711.
[29] N. Fujimura, T. Nishihara, S. Goto, J.F. Xu, T. Ito, Journal of Crystal Growth 130 (1993) 269.
[30] G.J. Exarhos, S.K. Sharma, Thin Solid Films 270 (1995) 27.
[31] X. Wen, W. Wu, Y. Ding, Z.L. Wang, Advanced Materials 25 (2013) 3371–3379.
[32] M.K. Puchert, P.Y. Timbrell, R.N. Lamb, Journal of Vacuum Science & Technology a-Vacuum Surfaces and Films 14 (1996) 2220.
[33] D. Raoufi, T. Raoufi, Applied Surface Science 255 (2009) 5812.
[34] S. Kim, W.I. Lee, E.H. Lee, S.K. Hwang, C. Lee, Journal of Materials Science 42 (2007) 4845.
[35] K. Ellmer, Journal of Physics D: Applied Physics 33 (2000) R17.
[36] T. Tsuji, M. Hirohashi, Applied Surface Science 157 (2000) 47.
[37] J. Nelson, The Physics of Solar Cells, Imperial College Press; Distributed by World Scientific Pub. Co., London; River Edge, NJ, 2003.
[38] Y.E. Lee, J.B. Lee, Y.J. Kim, H.K. Yang, J.C. Park, H.J. Kim, Journal of Vacuum Science & Technology a-Vacuum Surfaces and Films 14 (1996) 1943.
[39] J.J. Chen, Y. Gao, F. Zeng, D.M. Li, F. Pan, Applied Surface Science 223 (2004) 318.
[40] R.J. Hong, H.J. Qi, J.B. Huang, G.B. He, Z.X. Fan, J.A. Shao, Thin Solid Films 473 (2005) 58.
[41] M. Yuste, R.E. Galindo, I. Caretti, R. Torres, O. Sanchez, Journal of Physics D: Applied Physics45 (2012) 025303.

Xiaonan Wen received his B.S. degree in Physics from Peking University, China in 2010. He is currently a Ph.D. student in the School of Materials Science & Engineering, Georgia Institute of Technology. His research interests include synthesis of functional nanomaterials, energy harvesting using piezoelectric and triboelectric generators, self-powered nanosystems, piezoelectronics and piezo-optoelectronics based on ZnO, GaN etc. for novel transistors and devices and integration of novel transistors into functional systems.

Wenzhuo Wu received his B.S. in Electronic Information Science and Technology in 2005 from the University of Science and Technology of China (USTC), Hefei and his M. Eng. in Electrical and Computer Engineering from the National University of Singapore (NUS) in 2008. After working at Chartered Semiconductor Manufacturing in Singapore from 2007 to 2008, he began the doctoral research under the supervision of Prof. Zhong Lin Wang and received his Ph. D. from Georgia Institute of Technology in Materials Science and Engineering in 2013. He currently continues to work with Prof. Zhong Lin Wang as the postdoctoral fellow. Wenzhuo's research interests include synthesis, fabrication and integration of nanomaterials/devices; nanotechnology-enabled applications in energy harvesting/conversion/storage, electronics, optoelectronics, sensing and interfacing; piezotronics/piezo-phototronics; self-powered micro/nano-systems.

Zhong Lin (ZL) Wang received his Ph.D. from Arizona State University in physics. He now is the Hightower Chair in Materials Science and Engineering, Regents' Professor, Engineering Distinguished Professor and Director, Center for Nanostructure Characterization, at Georgia Tech. Dr. Wang has made original and innovative contributions to the synthesis, discovery, characterization and understanding of fundamental physical properties of oxide nanobelts and nanowires, as well as applications of nanowires in energy sciences, electronics, optoelectronics and biological science. His discovery and breakthroughs in developing nanogenerators established the principle and technological road map for harvesting mechanical energy from environment and biological systems for powering a personal electronics. His research on self-powered nanosystems has inspired the worldwide effort in academia and industry for studying energy for micro-nano-systems, which is now a distinct disciplinary in energy research and future sensor networks. He coined and pioneered the field of piezotronics and piezo-phototronics by introducing piezoelectric potential gated charge transport process in fabricating new electronic and optoelectronic devices. Details can be found at: http://dx.doi.org/www.nanoscience.gatech.edu.